

Identification of PN G232.0+05.7 as a new halo planetary nebula and of IRAS 19336-0400 as a new type III planetary nebula*

C. B. Pereira¹ and L. F. Miranda²

¹ Observatório Nacional-MCT, Rua José Cristino, 77. CEP 20921-400 São Cristóvão. Rio de Janeiro-RJ, Brazil
e-mail: claudio@on.br

² Instituto de Astrofísica de Andalucía, CSIC, Apdo. 3004, 18080 Granada, Spain
e-mail: lfm@iaa.es

Received 23 January 2007 / Accepted 15 March 2007

ABSTRACT

Aims. We determined the nature and Peimbert type of two low-excitation planetary nebulae, PNG 232.0+05.7 and IRAS 19336-0400.

Methods. We used low resolution optical spectroscopy in the range 3200–9000 Å.

Results. We derived line intensities, reddening, physical conditions (electron density and temperature) and ionic and elemental abundances. Based on the abundance analysis and its radial velocity we conclude that PNG 232.0+05.7 is a halo planetary nebulae. This discovery thus adds this object to the sample of ten known halo planetary nebulae. IRAS 19336-0400 is probably a type III planetary nebulae, as strongly suggested by its abundances and high radial velocity, although this conclusion awaits a better estimation of its distance.

Key words. planetary nebulae: individual: PN G232.0+05.7 – planetary nebulae: individual: IRAS 19336+0400

1. Introduction

The two objects analyzed in this work, PN G232.0+05.7 and IRAS 19336-0400, came to our attention for different reasons. In the case of PN G232.0+05.7 we were looking for whether in Table 1 of Sanduleak & Stephenson (1972) an object classified as a very low-excitation nebula, would have any information about the presence of absorption features in its spectrum. If so, this object could be a good target to be labelled as a “peculiar planetary nebula” as those singled out by Lutz (1977). In her study, she realize that there is a small group of objects in the Catalogue of Planetary Nebulae (Perek & Kohoutek 1967) that appear peculiar because they have nebular emission lines in combination with the absorption spectrum of a cool (spectral type A to K) central star.

To illustrate the connection between an object classified as a very low-excitation compact nebula and one that could might be called as “peculiar planetary nebula”, according to Lutz (1977), we could mention Hen 3-1312 (=SaSt 2-12, Sanduleak & Stephenson 1972). Pereira (2004) shows that Hen 3-1312 has a continuum spectrum of a F-type star with emission lines. Another example of a very low-excitation compact nebula, but instead, with a continuum of a hot star, is provided by the object Hen 2-138 (=SaSt 2-10, its spectrum is shown in Fig. 1).

Since our primary goal is to find an object which presents in its spectrum emission lines in combination with the absorption features of a cool star, we first need to observe spectroscopically a candidate in order to set what kind of very low-excitation compact nebula we are going to investigate. Therefore, we searched again Table 1 of Sanduleak & Stephenson (1972) and found that

PN G232.0+05.7 (=SaSt 2-3=MWC 574) could be a good candidate for this kind of investigation.

The other low-excitation object, IRAS 19336-0400, entered in our analysis in the framework of our spectroscopic survey of post-AGB candidates (Pereira & Miranda 2007). Our aim in that survey was to present and discuss the spectra of several candidates to post-AGB stars, in order to establish their nature and identify new post-AGB stars. Since the IRAS flux ratios for IRAS 19336-0400 are $F(12 \mu\text{m})/F(25 \mu\text{m}) = 0.05$ and $F(25 \mu\text{m})/F(60 \mu\text{m}) = 1.47$, IRAS 19336-0400 is located in the region of the proto-planetary nebula candidates in the IRAS [12]–[25] vs. [25]–[60] colour diagram (see Fig. 1 in Pereira & Miranda 2007). IRAS 19336-0400 was first identified as a emission-line object by Stephenson & Sanduleak (1977) and later spectroscopically observed by Downes & Keyes (1988). Its spectrum is described by Van de Steene et al. (1996) and Parthasarathy et al. (2000). They both suggest that IRAS 19336-0400 is a young and low-excitation planetary nebula with a B1 supergiant central star.

In this paper we present an abundance analysis of these two low-excitation objects, based on low resolution optical spectroscopy, carried out with the aim of investigating their nature in detail.

2. Observations and reduction

Spectroscopic observations were performed with CAFOS (Calar Alto Faint Object Spectrograph) attached to the 2.2 m telescope of the Calar Alto Observatory (Almería, Spain). IRAS 19336-0400 was observed on 2005 August 6 while PN G232.0+05.7 was observed on 2006 February 6. The detector was a SITe CCD with 2048 pixels in the spectral direction. The observations were done using the grisms B-100 and R-100 covering

* Based on observations collected at the Centro Astronomico Hispano Aleman (CAHA) at Calar Alto, operated jointly by the Max-Planck Institut für Astronomie and the Instituto de Astrofísica de Andalucía (CSIC).

Table 1. Observed emission lines in units of $H\beta = 100.0$.

Wavelength	Identification	$F(\lambda)$	
		PNG 232.0+05.7	IRAS 19336-0400
3727	[O II]	268.5	41.3
3838	He II		2.2
	H9		
3889	He I		4.4
	H8		
3968	H ϵ	7.7	6.8
	[Ne III]		
4101	H δ	24.5	14.2
4340	H γ	37.0	33.0
4861	H β	100.0	100.0
5007	[O III]	2.5	
5105	?		4.1
5202	[N I]		2.0
5754	[N II]	2.0	2.5
5876	He I	0.7	
6300	[O I]	0.5	4.0
6363	[O I]		1.7
6548	[N II]	39.0	98.0
6563	H α	326.5	578.0
6584	[N II]	107.5	300.0
6717	[S II]	4.0	12.8
6731	[S II]	5.6	26.1
7135	[Ar III]	0.5	
7320	[O II]	5.0	11.1
7330	[O II]	4.0	8.4
8446	O I		16.7
8467	P 17	0.6	1.4
8502	P 16	0.9	1.5
8545	P 15	1.0	2.4
8598	P 14	1.1	2.2
8665	P 13	1.2	3.2
8750	P 12	1.4	3.7
8862	P 11	2.0	4.4
9014	P 10	3.1	6.0
9069	[S III]	4.4	5.4
9229	P 9	4.6	11.4
9532	[S III]	17.6	37.6
9546	P 8	11.4	10.8
$F(H\beta)$	[erg/cm ² s]	2.1×10^{-13}	1.8×10^{-13}

the spectral range 3200–5800 Å and 5900–9000 Å, respectively. The slit orientation was North-South and the slit width was 2'' for IRAS 19336-0400 and 1'' for PN G232.0+05.7. Exposure time was 1500 s and 1200 s for IRAS 19336-0400 and PN G232.0+05.7, respectively. The sky conditions in these observations were mostly clear, but not photometric with a mean seeing of 1.5''. Spectrophotometric standards from Oke (1974) and Massey et al. (1988) were also observed. The spectra were reduced using standard IRAF tasks, from bias subtraction and flat-field correction, through spectral extraction and wavelength and flux calibration.

The flux of the emission lines was measured by the conventional method, adjusting a Gaussian function to the line profile, thereby obtaining the intensity, the central wavelength and the line width at half power level. Uncertainties in the line intensities come mainly from the position of the underlying continuum. We estimate the flux error to be about 20% for the weak lines (line fluxes ≈ 10 on the scale of $H\beta = 100$) and about 10% for stronger lines. Table 1 shows the observed line intensities. Relative intensities for PN G232.0+05.7 and IRAS 19336-0400 in Table 1 are in reasonable agreement with those given by Dopita & Hua (1997) and van de Steene et al. (1996), respectively.

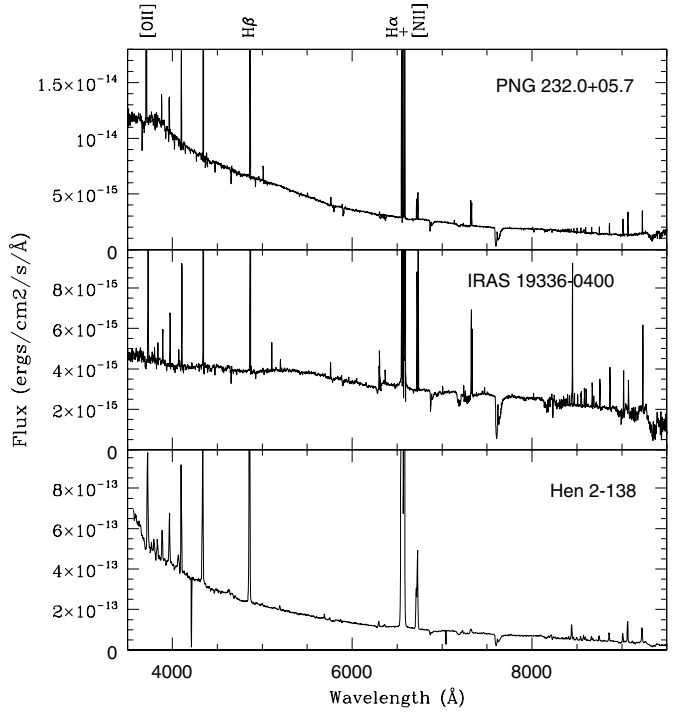


Fig. 1. Observed spectra of PNG 232.0+05.7 and IRAS 19336-0400. We also show the spectrum of the other low-excitation planetary nebula Hen 2-138.

Figure 1 shows the observed spectra of the two sources analyzed in this work. The spectra of PNG 232.0+05.7 and IRAS 19336-0400 are typical of low-excitation planetary nebulae where the intensity of the [O II] 3727 Å line is comparable to or even stronger than that of $H\beta$. In addition, despite the presence of strong [O II], the [O III] 5007 Å line is weaker than $H\beta$ or even absent, thus indicating an exceptionally low excitation in the nebular component of the spectrum. Helium absorption features can also be identified in both objects and, in the case of PNG 232.0+05.7, the C IV 14658 Å absorption is also observed. Figure 1 also shows the spectrum Hen 2-138, another low-excitation planetary nebula, for comparison.

3. Data analysis

3.1. Extinction

We derive the extinction for the two sources from the observed Balmer decrement assuming Case B recombination (the dereddened relative strength of $H\alpha/H\beta = 2.86$; Hummer & Storey 1987; $N_e = 1000 \text{ cm}^{-3}$ and $T_e = 10000 \text{ K}$). Table 2 provides the value of the $E(B-V)$ obtained for such procedure. Previous determination of the extinction $E(B-V)$ value for IRAS 19336-0400 is 0.53 (van de Steene et al., 1996) which is close agreement with ours. For PN G232.0+05.7 Tylenda et al. (1992) and Dopita & Hua (1997) obtained $E(B-V)$ values of 0.75 and 0.27, respectively. The differences between these values and ours are probably due to the observing conditions, such as seeing and slit width.

3.2. Electron temperature and density

Nebular electron temperature and density were estimated using the IRAF routine TEMDEN, version 2.0 (Shaw & Dufour 1995). Electron density was obtained from the [S II] 6717/6731 line

Table 2. Physical parameters and abundances for IRAS 19336-0400 and PN G232.0+05.7

Physical parameters		
	IRAS 19336-0400	PNG 232.0+05.7
$E(B - V)$	0.55 ± 0.03	0.11 ± 0.02
$N_e(\text{[S II]}) (\text{cm}^{-3})$	$13\,000 \pm 3600$	$2\,100 \pm 600$
$T_e(\text{[N II]})$	$7\,600 \pm 600 \text{ K}$	$9\,600 \pm 930 \text{ K}$
Ionic abundances		
	IRAS 19336-0400	PNG 232.0+05.7
N^+ (6584Å)	8.47×10^{-5}	2.42×10^{-5}
O^0 (6300Å)	1.45×10^{-6}	—
O^+ (3727Å)	3.26×10^{-4}	1.87×10^{-4}
O^{++} (5007Å)	—	1.22×10^{-6}
S^+ (6731Å)	3.11×10^{-6}	3.00×10^{-7}
Elemental abundances		
$N(\text{O})/N(\text{H})$	3.6×10^{-4}	1.9×10^{-4}
$N(\text{N})/N(\text{H})$	8.4×10^{-5}	2.9×10^{-5}
$N(\text{S})/N(\text{H})$	3.1×10^{-6}	3.0×10^{-7}

ratio and electron temperature from the [N II] (6548+6584)/5754 ratio. The values are given in Table 2.

3.3. Ionic and elemental abundances

Ionic and elemental abundances were obtained using the IRAF routine *NEBULAR*, version 2.0 (Shaw & Dufour 1995). Final elemental abundances were computed by adding the abundances of the observed ions for an element and then multiplying this sum by the ionization factors (ICFs) taken from Kwinter & Henry (2001). Table 2 also shows the results. The uncertainties in ionic and elemental abundances are estimated to be $\pm 30\%$.

4. Discussion

4.1. PN G232.0+05.7 as a halo planetary nebula

According to Peimbert (1990), planetary nebulae can be divided into four categories that are distinguished by their chemical compositions and kinematical properties. In brief, type I planetary nebulae are defined by $\text{N}/\text{O} \geq 0.5$ and $\text{He}/\text{H} \geq 0.125$. They are often bipolar and believed to have evolved from intermediate mass stars. Type II planetary nebulae are defined as intermediate population objects with scale heights $|z|$ less than 1 kpc and without helium and nitrogen enrichments. Type III planetary nebulae are not members of the halo population and present $|\Delta_{\text{pr}} V| \geq 60 \text{ km s}^{-1}$, where $|\Delta_{\text{pr}} V|$ is the peculiar radial velocity relative to the galactic rotation, that is, the difference between the observed radial velocity and that expected on the basis of circular galactic orbit. Finally, type IV planetary nebulae are those that belong to the halo population, with $|\Delta_{\text{pr}} V| \geq 60 \text{ km s}^{-1}$ and $\log(\text{O/H}) + 12 \leq 8.1$.

In Table 3 we list the average abundance for the same elements studied here, based on some studies of planetary nebulae, in comparison with our two analyzed objects.

By comparing the chemical composition of PN G232.0+05.7 with other type of planetary nebulae (Table 3), it is clear that PNG 232.0+05.7 has an abundance pattern which is very similar to that of other halo planetary nebulae. In particular, the elements studied here present low abundances when compared with other type of planetary nebulae. In Fig. 2 we plot a $12+\log(\text{S}/\text{H})$ vs. $12+\log(\text{O}/\text{H})$ diagram for a sample of types I, II, III and IV planetary nebulae. This diagram provides more indication that PNG 232.0+05.7 is a halo planetary nebula. Its position in such

Table 3. Average planetary nebulae abundances.

	$\log \epsilon(\text{N})$	$\log \epsilon(\text{O})$	$\log \epsilon(\text{S})$	$(\text{S}/\text{O}) \times 10^3$
Type I ^a	8.76 ± 0.22	8.76 ± 0.08	6.96 ± 0.22	0.16 ± 0.08
Type II ^a	8.20 ± 0.26	8.71 ± 0.17	6.78 ± 0.43	0.12 ± 0.09
Type III ^{b,c}	8.00	8.47 ± 0.23	6.66 ± 0.29	0.18 ± 0.29
Type IV ^{a,d,e}	7.46 ± 0.47	8.06 ± 0.27	5.91 ± 0.66	0.06 ± 0.07
PNG 232.0+05.7	7.38 ± 0.14	8.27 ± 0.14	5.48 ± 0.14	0.02 ± 0.01
IRAS 19336-0400	7.92 ± 0.12	8.53 ± 0.13	6.48 ± 0.14	0.09 ± 0.04

^a: Henry et al. (2004). ^b: Peimbert (1990). ^c: Maciel & Köppen (1994). ^d: Peimbert (1980). ^e: Howard et al. (1997).

Table 4. Radial velocities and galactic latitudes of halo planetary nebulae

Objects	$RV (\text{km s}^{-1})$	b°	Reference
PNG 232.0+05.7	+166	+5.7	1
	+145		2
NGC 2242	+20	+15.9	3
NGC 4361	+9.6	+43.6	3
M 2-29	-103	-0.03	3
H 4-1	-141	+88.1	3
BB-1	+196	-76.2	3
DDDM-1	-304	+41.4	4
K 648	-141	-27.1	5
GJIC-1	-15.3	-7.5	6

(1) Durand et al. (1998). (2) Dopita & Hua (1997). (3) Torres-Peimbert et al. (1990). (4) Clegg et al. (1987). (5) Howard (1997). (6) Gillett et al. (1989).

abundance diagram is close to the position of the three halo planetary nebulae K 648, BB-1 and H 4-1.

The nature of PN G232.0+05.7 as a halo object is further indicated when its peculiar velocity is examined. Table 4 presents the radial velocities of some known halo planetary nebulae. The $|\Delta_{\text{pr}} V|$ for PN G232.0+05.7 is $65\text{--}85 \text{ km s}^{-1}$ where we used for the distance of PN G232.0+05.7 a value of 4 kpc (Gesicki et al. 2006) and the galactic rotation curve of Ostriker & Caldwell (1983). We also note that the deduced value does not critically depend on the distance in the range of 2–6 kpc. Finally, we also list in Table 4 the galactic latitude of the type IV planetary nebulae. PN G232.0+05.7 presents a relatively low galactic latitude. However, other halo planetary nebulae also present a similar value.

All these findings show that PN G232.0+05.7 is a halo planetary nebula. This discovery thus adds this object to the sample of ten known halo planetary nebula (Howard et al. 1997).

4.2. IRAS 19336-0400: a type III planetary nebula?

Figure 2 shows the position of IRAS 19336-0400 in the abundance diagram. From this diagram alone, it is not possible to settle unambiguously to which type IRAS 19336-0400 belongs. However, when the abundances of IRAS 19336-0400 are compared with the average abundances of all types of planetary nebulae (Table 3), then IRAS 19336-0400 is suspected to belong to type III. As already mentioned, type III planetary nebulae should also present $|\Delta_{\text{pr}} V| \geq 60 \text{ km s}^{-1}$. Because no published value exists for the radial velocity of IRAS 19336-0400, we deduce it from the intensity peak of the emission lines in our spectrum and found $203 \pm 34 \text{ km s}^{-1}$. The high radial velocity strongly suggests that IRAS 19336-0400 also fulfills the kinematical constraint of type III planetary nebulae. Nevertheless, the lack of any estimate for the distance to IRAS 19336-0400 does not make it possible to obtain its peculiar radial velocity.

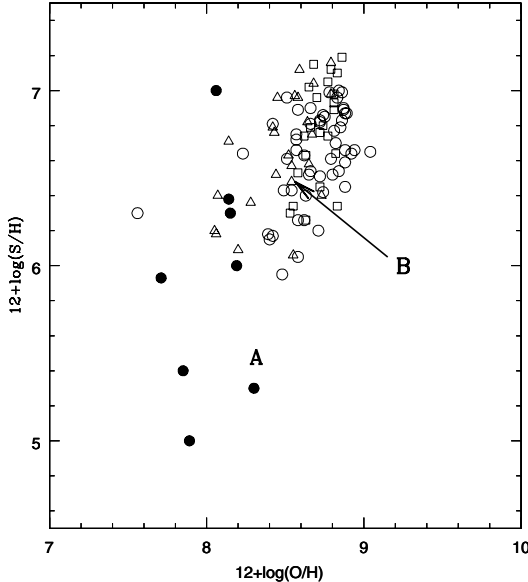


Fig. 2. Plot of $12+\log(\text{S}/\text{H})$ vs. $12+\log(\text{O}/\text{H})$ for a sample of type I (open squares), type II (open circles), type III (open triangles) and type IV planetary nebulae (filled circles) from Henry et al. (2004), Maciel & Köppen (1994) and Howard et al. (1997). The position of PN G232.0+05.7 is labelled by A and that of IRAS 19336-0400 by the arrow B.

There still remains the question whether IRAS 19336-0400 is a young planetary nebula or a hot post-AGB star. From our data we cannot provide a definitive answer, due to the presence of emission lines. We measured the strength of some helium absorption lines in the spectrum of IRAS 19336-0400 and in other stars in the library spectra of Jacoby et al. (1984) and we conclude that the absorption spectrum of IRAS 19336-0400 probably corresponds to a B supergiant star, in agreement with previous determinations (Van de Steene et al. 1996; Parthasarathy et al. 2000). This implies that the exciting star of IRAS 19336-0400 is still in the post-AGB phase. On the other hand, Van de Steene et al. (1996) point out the possibility that the central star of IRAS 19336-0400 is a binary. If this is the case, the B supergiant would be the companion of the true central star that would probably present a relatively low effective temperature according to the very low-excitation nebular spectrum. Only after high resolution spectroscopic observations have been employed, one will be able to constraint the nature of IRAS 19336-0400.

5. Conclusions

The main conclusions from our spectroscopic analysis of PN G232.0+05.7 and IRAS 19336-0400, employing low resolution optical spectra, can be summarized as follows:

1. PN G232.0+05.7 is a halo planetary nebula. This conclusion is supported by its elemental abundances as well as

by its position in the abundance diagram $12+\log(\text{S}/\text{H})$ vs. $12+\log(\text{O}/\text{H})$. Its high radial velocity and the value of $|\Delta_{\text{pr}} V|$ give further support the halo nature of PN G232.0+05.7. PN G232.0+05.7 thus adds to the list of ten known halo planetary nebulae.

2. IRAS 19336-0400 is probably a type III planetary nebula, as indicated by the abundance analysis for the elements studied here. The high radial velocity deduced from our spectrum also points to a type III planetary nebula, although the lack of a value for the distance to IRAS 19336-0400 does not allow us to estimate its peculiar radial velocity. The absorption spectrum suggests that the central star of IRAS 19336-0400 is still in the post-AGB phase. However, the possibility of a binary nature cannot be ruled out.

Acknowledgements. We thank our referee (Franco Sabbadin) for detailed comments that have improved the presentation and interpretation of the data. We thank the Calar Alto Observatory for allocation of director's discretionary time to observe PNG 232.0+05.7. We are very grateful to the staff of the Calar Alto Observatory for assistance in the observations. We also thank Karen Kwitter for providing us with the spectrum of Hen 2-138. This work has been supported partially by grant AYA2005-01495 of the Spanish MEC (co-funded by FEDER funds). LFM is also supported by Junta de Andalucía.

References

- Clegg, R. E. S., Peimbert, M., & Torres-Peimbert, S. 1987, MNRAS, 224, 761
- Dopita, M. A., & Hua, C. T. 1997, ApJS, 108, 515
- Downes, R. A., & Keyes, C. D. 1988, AJ, 96, 777
- Durand, S., Acker, A., & Zijlstra, A. 1998, A&AS, 132, 13
- Gesicki, K., Zijlstra, A. A., Acker, A., et al. 2006, A&A, 451, 925
- Gillet, F. C., Jacoby, G. H., Joyce, R. R., et al. 1989, ApJ, 338, 86
- Henry, R. B. C., Kwitter, K. B., & Balick, B. 2004, AJ, 127, 2284
- Howard, J. W., Henry, R. B. C., & McCartney, S. 1997, MNRAS, 284, 465
- Hummer, D. G., & Storey, P. J. 1987, MNRAS, 224, 801
- Jacoby, G. H., Hunter, D. A., & Christian, C. A. 1984, ApJS, 56, 257
- Kwitter, K. B., & Henry, R. B. C. 2001, ApJ, 562, 804
- Lutz, J. H. 1977, A&A, 60, 93
- Maciel, W. J., & Koppen, J. 1994, A&A, 282, 436
- Massey, P., Strobel, K., Barnes, J. V., & Anderson, E. 1988, ApJ, 328, 215
- Oke, J. B. 1974, ApJS, 27, 21
- Ostriker, J. P., & Caldwell, J. A. R. 1983, in Kinematics, Dynamics, and Structure of the Milky Way, ed. W. L. H. Shuter (Dordrecht: Reidel), p. 249
- Parthasarathy, M., Acker, A., & Stenholm, B. 1998, A&A, 329, L9
- Parthasarathy, M., Vijapurkar, J., & Drilling, J. S. 2000, A&AS, 145, 269
- Peimbert, M. 1990, Rep. Prog. Phys., 53, 1559
- Pereira, C. B. 2004, A&A, 413, 1009
- Pereira, C. B., & Miranda, L. F. 2007, A&A, 462, 231
- Perek, L., & Kohoutek, L. 1967, Catalogue of Galactic Planetary Nebulae, Czechoslovak Academy of Sciences, Prague
- Sanduleak, N., & Stephenson, C. B. 1972, ApJ, 178, 183
- Shaw, R. A., & Dufour, R. J. 1995, PASP, 107, 896
- Stephenson, C. B., & Sanduleak, N. 1977, ApJS, 33, 459
- Torres-Peimbert, S., Peimbert, M., & Pena, M. 1990, A&A, 233, 540
- Van de Steene, G. C., Jacoby, G. H., & Pottasch, S. R. 1996, A&AS, 118, 243
- Vijapurkar, J., Driling, J. S., & Parthasarathy, M. 1997, AJ, 114, 1573